

## Pressure-induced changes in transport properties of layered $\text{La}_{1.2}\text{Ca}_{1.8}\text{Mn}_2\text{O}_7$

K. V. Kamenev,\* M. R. Lees, G. Balakrishnan, and D. McK. Paul  
*Department of Physics, University of Warwick, Coventry CV4 7AL, United Kingdom*  
 (Received 14 July 1997)

The transport properties of a single crystal of  $\text{La}_{1.2}\text{Ca}_{1.8}\text{Mn}_2\text{O}_7$  with the layered  $\text{Sr}_3\text{Ti}_2\text{O}_7$ -type perovskite structure have been studied under hydrostatic pressures of up to  $\sim 9$  kbar. It is found that  $\text{La}_{1.2}\text{Ca}_{1.8}\text{Mn}_2\text{O}_7$  undergoes a first-order phase transition from a paramagnetic insulating to a low-temperature ferromagnetic metallic state which is accompanied by a large decrease in the electrical resistivity. At ambient pressure the magnetic phase transition takes place at  $T_c = 242$  K and as the external pressure is applied the critical temperature increases linearly at a rate of 1.1 K/kbar. The present results reflect the competition between double and superexchange resulting from two-dimensional Mn-O-Mn networks and can be interpreted in terms of the exchange striction model. [S0163-1829(97)51044-7]

The two-dimensional material  $\text{La}_{1.2}\text{Ca}_{1.8}\text{Mn}_2\text{O}_7$  belongs to the series of perovskite oxides with the general formula  $(R_{1-x}A_x)_{n+1}\text{Mn}_n\text{O}_{3n+1}$ , where  $R$  is a rare-earth ion and  $A$  is a divalent cation. Doping with  $A$  introduces a mixed valence of  $\text{Mn}^{3+}$  and  $\text{Mn}^{4+}$  ions creating the conditions for the appearance of a metallic state due to coupling between the charge carriers and localized spin moments.<sup>1,2</sup> The general formula implies that the structure is composed of the  $(R_{1-x}A_x)_2\text{O}_2$  NaCl-type block layers separated by  $n$   $\text{MnO}_2$  sheets.<sup>3</sup> The  $n = \infty$  case corresponds to the three-dimensional structure of the  $(R_{1-x}A_x)\text{MnO}_3$  perovskites, which have been extensively studied recently due to the large negative magnetoresistance occurring near the magnetic phase transition.

The layered structures with finite  $n$  present the possibility of studying anisotropic exchange with basically the same interactions in the  $(R_{1-x}A_x)_2\text{O}_2$  layers. Separating the layers by a different number of  $\text{MnO}_2$  sheets can lead to a change in the ground state of the electronic system. For the series of  $(\text{La}_{1-x}\text{Sr}_x)_{n+1}\text{Mn}_n\text{O}_{3n+1}$  perovskites the single-sheet ( $n = 1$ ) compound (a  $\text{K}_2\text{NiF}_4$ -type structure) is a nonmetallic ferromagnet<sup>4,5</sup> while the double-sheet  $(\text{La}_{1-x}\text{Sr}_x)_3\text{Mn}_2\text{O}_7$ ,  $x = 0.6$  (a  $\text{Sr}_3\text{Ti}_2\text{O}_7$ -type) is a conducting ferromagnet.<sup>3,6</sup> Recently, it was found that the pressure variation of the length of the distinguishable manganese-oxygen bonds within and between  $\text{MnO}_2$  sheets have different signs.<sup>7</sup> This conclusion is in contrast to that found for three-dimensional perovskite structures where the pressure-driven changes in structure result in a tilting of the "rigid"  $\text{MnO}_6$  octahedra.<sup>8,9</sup> In this paper we report on the effect of pressure on the transport properties of the  $(\text{La}_{1-x}\text{Ca}_x)_{n+1}\text{Mn}_n\text{O}_{3n+1}$  ( $x = 0.6$ ) compound.

Single crystals of  $\text{La}_{1.2}\text{Ca}_{1.8}\text{Mn}_2\text{O}_7$  were grown from polycrystalline rods in an infrared image furnace using the floating-zone method. The precursor materials were prepared by mixing stoichiometric amounts of  $\text{La}_2\text{O}_3$ ,  $\text{CaCO}_3$ , and  $\text{MnO}_2$ . The powder was ground and calcined twice at  $1350^\circ\text{C}$  for 16 h and then pressed into rods which were sintered at  $1370^\circ\text{C}$  for 16 h. To characterize the single crystals a tiny piece of crystal was ground to powder and checked with x-ray diffraction. The x-ray diffraction pattern

for the powder is presented in Fig. 1. The diffraction peaks are indexed with respect to the  $\text{Sr}_3\text{Ti}_2\text{O}_7$ -type structure. The space group is  $I4/mmm$  with the lattice parameters of the tetragonal unit cell being  $a = 3.844 \text{ \AA}$  and  $c = 19.131 \text{ \AA}$ . Good agreement between the calculated and observed positions and intensities of the lines indicates that the sample is a single phase of the  $\text{Sr}_3\text{Ti}_2\text{O}_7$  type.

The electrical resistivity was measured by standard four-point technique with the contacts glued on a bar-shaped sample with silver-based epoxy. The pressure measurements were performed in a CuBe pressure cell with a fixed hydrostatic pressure of up to 9 kbar. Fluorinert FC-77 was used as a pressure-transmitting medium. Pressure and temperature were measured using a calibrated manganin sensor and a Cernox resistor CX-1030-AA, respectively.

The temperature dependencies of the ac susceptibility  $\chi$

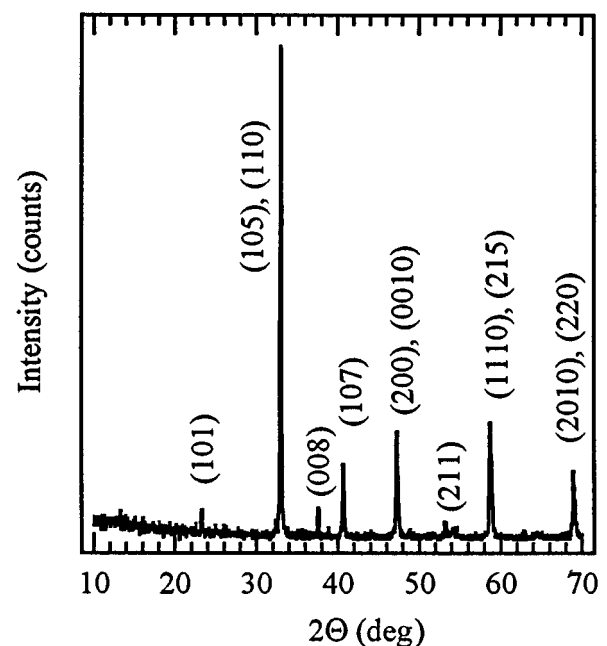


FIG. 1. X-ray diffraction pattern of a  $\text{La}_{1.2}\text{Ca}_{1.8}\text{Mn}_2\text{O}_7$  powder sample.

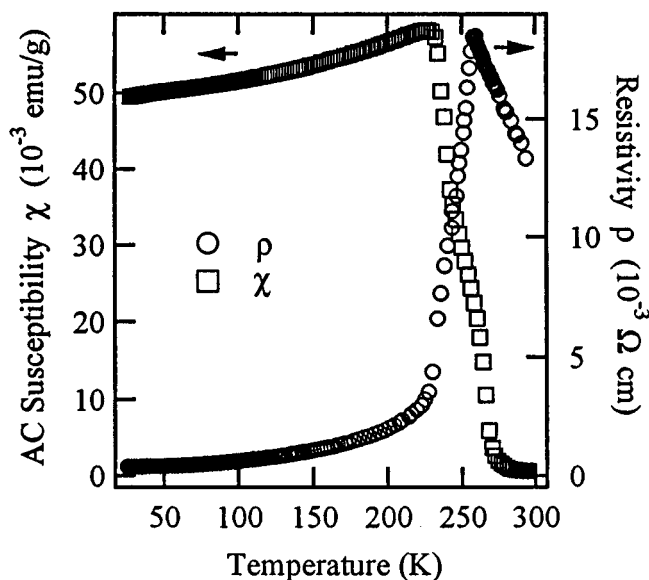


FIG. 2. Temperature dependence of the ac susceptibility  $\chi$  and electrical resistivity  $\rho$  at ambient pressure (data collected during a heating run).

and electrical resistivity  $\rho$  are presented in Fig. 2. The sharp change in the temperature behavior of  $\rho$  indicates that the sample undergoes a phase transition at 242 K on heating from a low-temperature metallic to high-temperature state with an activated temperature dependence. A temperature hysteresis discovered during cooling-heating runs shows that the phase transition is of the first order. The decrease in  $\chi$  around 250 K marks a transition from a magnetically ordered to a paramagnetic state (PM). The value of  $\chi = 5.8 \times 10^{-2}$  emu/g is of the same order of magnitude as the ac susceptibilities of the ferromagnetically ordered Ca-doped manganese perovskites  $\text{Pr}_{1-x}\text{Ca}_x\text{MnO}_3$  (Ref. 10), which indicates that the low-temperature phase is ferromagnetic (FM). A positive value for the Curie-Weiss temperature  $\Theta_{\text{CW}}$  extracted from  $\chi^{-1}$  vs  $T$  above the Curie temperature also suggests that the system orders ferromagnetically. Interestingly, the three-dimensional  $\text{La}_{0.4}\text{Ca}_{0.6}\text{MnO}_3$  is an antiferromagnetic insulator,<sup>11</sup> while  $\text{La}_{1.2}\text{Ca}_{1.8}\text{Mn}_2\text{O}_7$  with the same level of Ca doping, i.e.,  $\text{Mn}^{3+}/\text{Mn}^{4+} = \frac{2}{3}$ , is a metallic ferromagnet. Thus, the character of low-temperature ordering can be switched from antiferromagnetic to ferromagnetic by introducing some extra sheets of  $\text{MnO}_2$  into the perovskite structure. The phase transition to the ferromagnetic phase is accompanied by a sharp decrease in electrical resistivity at  $T_c = 242$  K (Fig. 2). This enabled us to determine the Curie temperature by the maximum of the temperature derivative of the resistivity. Such coincident magnetic and associated electronic transitions are common in magnetoresistive materials. They have already been observed in three-dimensional Ca-doped  $\text{La}_{1-x}\text{Ca}_x\text{MnO}_3$  (Ref. 11) and in layered  $(\text{La}_{1-x}\text{Sr}_x)_3\text{Mn}_2\text{O}_7$  compounds.<sup>3,6,12</sup> This is in contrast to the results on  $\text{La}_{1.5}\text{Ca}_{1.5}\text{Mn}_2\text{O}_7$ , where the insulator-metal phase transition occurs some 120 K below the magnetic phase transition.<sup>9</sup>

A set of the curves presenting the temperature dependence of  $\rho$  for heating runs at several pressures is shown in Fig. 3.

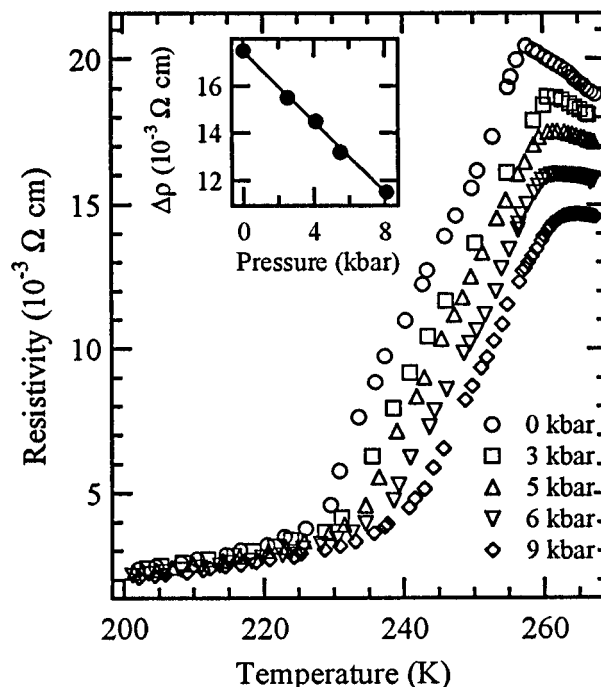


FIG. 3. Temperature dependence of the electrical resistivity  $\rho$  at different pressures. Inset:  $\Delta\rho = \rho_{T=260\text{ K}} - \rho_{T=210\text{ K}}$  vs pressure; actual pressure is calculated at  $T = 260$  K.

It should be noted that because of differences in the thermal expansion coefficients of the pressure-transmitting medium and the pressure cell, the pressure inside the cell decreases as the temperature is lowered. The actual pressure at a given temperature can be calculated from the electrical resistivity of the calibrated manganin sensor. The curves in Fig. 3 are marked according to the starting pressures of 0, 3, 5, 6, and 9 kbar at room temperature. The applied pressure reduces the electrical resistivity in the high-temperature paramagnetic state; however,  $\rho$  is almost pressure independent in the metallic ferromagnetic region. This results in a decrease in the change in resistivity which accompanies the magnetic phase transition. In the inset in Fig. 3 we present the pressure dependence of  $\Delta\rho$  which is the difference between the resistivity  $\rho_{T=260\text{ K}}$  in the paramagnetic phase at 260 K and  $\rho_{T=210\text{ K}}$  in the ferromagnetic state at 210 K.  $\Delta\rho$  decreases linearly with applied pressure giving the ratio  $d(\Delta\rho)/dP = -7.4 \times 10^{-4}$  ( $\Omega\text{ cm}$ )/kbar. Such a decrease in resistivity can be related to the anisotropic compressibility found recently in the layered  $\text{La}_{1.2}\text{Ca}_{1.8}\text{Mn}_2\text{O}_7$  compound, which exhibits a similar magnetic phase transition.<sup>6,7</sup> There are two distinguishable Mn-O bonds parallel to the fourfold  $c$  axis of the  $I4/mmm$  symmetry group. One of them binds the Mn atom of the  $\text{MnO}_2$  plane to the oxygen ion within the plane [Mn-O(1)], while the other binds the Mn atom to an oxygen ion located between the planes [Mn-O(2)]. When hydrostatic pressure is applied to the sample in the high-temperature paramagnetic state, the Mn-O(1) bonds contract while the Mn-O(2) bonds expand.<sup>7</sup> This can lead to an increased overlap between the adjacent electronic orbitals of manganese ions in  $\text{MnO}_2$  planes. We suggest that the above mechanism is responsible for the enhanced ‘‘in-plane’’ conductivity.

The results of the present study are summarized in the

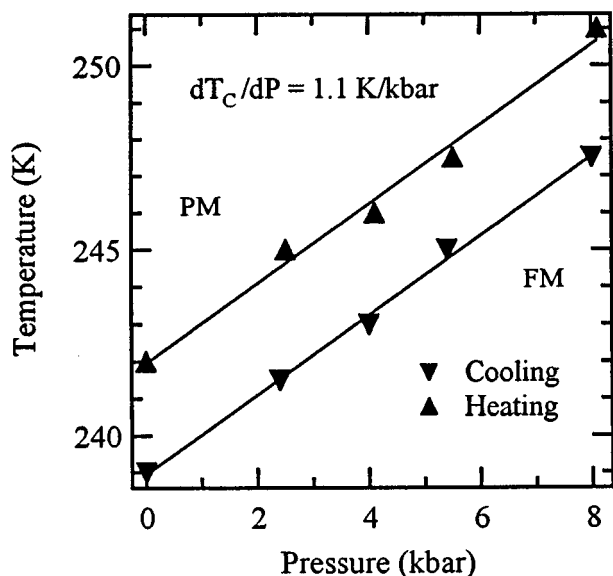


FIG. 4. Magnetic pressure-temperature phase diagram of  $\text{La}_{1.2}\text{Ca}_{1.8}\text{Mn}_2\text{O}_7$ . The actual values of pressure are calculated at  $T_c$ .

magnetic  $P$ - $T$  phase diagram of  $\text{La}_{1.2}\text{Ca}_{1.8}\text{Mn}_2\text{O}_7$  presented in Fig. 4. The Curie temperature  $T_c$  increases under applied pressure at a rate of 1.1 K/kbar for cooling as well as for heating runs. A qualitative explanation of the positive pressure dependence of the Curie temperature can be given in terms of the exchange striction model recently discussed in Ref. 7. Using the neutron diffraction data for  $\text{La}_{1.2}\text{Ca}_{1.8}\text{Mn}_2\text{O}_7$  under pressure, Argyriou *et al.* have shown that at low temperatures the spins of neighboring manganese atoms are ordered ferromagnetically within each  $\text{MnO}_2$  plane but exhibit a nonzero cant angle  $\Theta$  for the coupling between planes.

The canted magnetic order arises from the competition between the interactions provided by the  $t_{2g}e_g$  electronic configuration of the Mn atoms. The electrons in the half-filled  $t_{2g}$  band are localized near the Mn ion sites and participate in *antiferromagnetic*  $\pi$  bonding. The  $e_g$  electrons are hybridized with the oxygen  $2p$  states creating chemical Mn-O-Mn bonds. Chemical substitution of  $\text{La}^{3+}$  by divalent  $\text{Sr}^{2+}$  introduces  $\text{Mn}^{4+}$  ions into the lattice and holes into the  $e_g$  band. This double exchange  $e^1-p_\sigma-e^0$  interaction between the  $\text{Mn}^{3+}$  and the  $\text{Mn}^{4+}$  ions favors a *ferromagnetic* spin coupling. Compressibility data for  $\text{La}_{1.2}\text{Sr}_{1.8}\text{Mn}_2\text{O}_7$  reveal that below  $T_c$  the compressibilities of the Mn-O(1) and Mn-O(2) bonds reverse their signs. The Mn-O(2) bond contracts under applied pressure while the Mn-O(1) bond expands, adjusting its length to preserve the equilibrium bond-length sum for the manganese ion. Due to the larger overlap integral for the  $e^1-p_\sigma-e^0$  component, the  $\sigma$ -bonding interactions tend to align the magnetic moments in the neighboring layers ferromagnetically decreasing the cant angle  $\Theta$  under pressure. This leads to an increase in the magnetic moment on Mn sites and to a positive value of  $dT_c/dP$  that we observe in  $\text{La}_{1.2}\text{Ca}_{1.8}\text{Mn}_2\text{O}_7$ .

In conclusion, we have presented results on the transport properties of layered perovskite  $\text{La}_{1.2}\text{Ca}_{1.8}\text{Mn}_2\text{O}_7$  under pressure. We have found that  $\text{La}_{1.2}\text{Ca}_{1.8}\text{Mn}_2\text{O}_7$  is a ferromagnet below  $T_c = 242$  K at ambient pressure. The magnetic phase transition to a ferromagnetic phase is accompanied by a large decrease in the electrical resistivity. Applied pressure lowers the electrical resistivity in the paramagnetic phase due to the anisotropic compressibility of the two-dimensional Mn-O-Mn networks. The magnetic  $P$ - $T$  phase diagram has been presented showing a positive pressure dependence of the Curie temperature. These phenomena can be understood in terms of the exchange striction model.

This work was supported by EPSRC Grant No. GR/K95802.

\*Author to whom correspondence should be addressed. FAX: (44) 1203 692016. Electronic address: phsch@csv.warwick.ac.uk

<sup>1</sup>C. Zener, *Phys. Rev.* **82**, 403 (1951).

<sup>2</sup>P.-G. de Gennes, *Phys. Rev.* **118**, 141 (1960).

<sup>3</sup>Y. Moritomo, A. Asamitsu, H. Kuwahara, and Y. Tokura, *Nature (London)* **380**, 141 (1996).

<sup>4</sup>Y. Moritomo, T. H. Arima, and Y. Tokura, *J. Phys. Soc. Jpn.* **64**, 4117 (1995).

<sup>5</sup>Y. Moritomo, Y. Tomioka, A. Asamitsu, Y. Tokura, and Y. Matsui, *Phys. Rev. B* **51**, 3297 (1995).

<sup>6</sup>J. F. Mitchell, D. N. Argyriou, J. D. Jorgensen, D. G. Hinks, C. D. Potter, and S. D. Bader, *Phys. Rev. B* **55**, 63 (1997).

<sup>7</sup>D. N. Argyriou, J. F. Mitchell, J. B. Goodenough, O. Chmaissem, S. Short, and J. D. Jorgensen, *Phys. Rev. Lett.* **78**, 1568 (1997).

<sup>8</sup>R. Mahesh, R. Mahendiran, A. K. Raychaudhuri, and C. N. R. Rao, *J. Solid State Chem.* **120**, 204 (1995).

<sup>9</sup>H. Asano, J. Hayakawa, and M. Matsui, *Appl. Phys. Lett.* **68**, 3638 (1996).

<sup>10</sup>M. R. Lees, J. Barratt, G. Balakrishnan, D. McK. Paul, and C. D. Dewhurst, *J. Phys.: Condens. Matter* **8**, 2967 (1996).

<sup>11</sup>P. Schiffer, A. P. Ramirez, W. Bao, and S.-W. Cheong, *Phys. Rev. Lett.* **75**, 3336 (1995).

<sup>12</sup>R. Mahesh, R. Mahendiran, A. K. Raychaudhuri, and C. N. R. Rao, *J. Solid State Chem.* **122**, 448 (1996).